Phosphorus Doping on FeNC and CNx Catalysts in Oxygen Reduction Reaction in PEM Acidic Media

Honors Thesis for Graduation with Distinction
Submitted 4/19/2016
By Kyle Qian

The Ohio State University
Department of Chemical and Biomolecular Engineering
140 West 19th Avenue
Columbus, OH 43210

Honors Committee:
Professor Umit S. Ozkan, Advisor
Professor James Rathman

Acknowledgements

I would like to thank everyone who has supported me in this project. I would like to thank the Heterogeneous Catalysis Research Group (HCRG). Dr. Umit S. Ozkan welcomed me and gave me this opportunity to explore the field of research and more about my capabilities and interests. This opportunity provided me with invaluable experience that I would never forget. I would also like to thank Kuldeep Mamtani and Deeksha Jain for their mentorship. They have taught me the value of teamwork, mental toughness to get through struggles, and have guided me to the completion of this project. Lastly, I would like to thank everyone else in the group who have helped me. I am grateful for what HCRG has done for me and I wish them the best in the future.

Abstract

Fuel cells catalysts are being researched to achieve higher activity and lower costs for oxygen reduction reaction. Iron nitrogen carbon (FeNC) and nitrogen carbon (CNx) catalysts hold promising potential for being catalytically active at low costs. Phosphorus was doped on both FeNC and CNx catalysts to improve activity because of phosphorus' elemental properties. The specific amount of phosphorus doping was also researched for activity optimization. Triphenylphosphine was used as a phosphorus dopant and incorporated in the ballmilling step for both FeNC and CNx synthesis. Activity testing using Rotating Disk Electrode (RDE) apparatus with glassy carbon working electrode was done on both FeNC and CNx catalysts with and without P-doping. The CV curves obtained from the testing in phosphoric acid acidic mediums were analyzed via onset or half-wave potentials to determine the catalytic activities. The results showed that P-doping did not positively affect the activity of FeNC but did positively affect the activity of CNx. The results suggest the different effectiveness of P-doping on different carbon structured catalysts.

Table of Contents

List of Figures

1. Introduction

To meet the increased demand for energy in the world that is focused on the direction of renewable alternative energy to replace limited natural reserves energy source as such petroleum, one of the biggest challenges is the development of technologies that provide inexpensive energy. Hydrogen has become an apparent energy source for the future since it can be converted from renewable sources in many ways (1). Fuel cell is one of the most promising candidates for reliable and efficient conversion of hydrogen into electric power in automotive and portable electronic applications on a large scale (2,3).

Fuel cells currently power buildings, factories, submarines, vehicles, and even portable devices such as laptops. A fuel cell system running on hydrogen has many advantages. It can be compact and lightweight, have no major moving parts, and achieve up to 99.99% reliability in ideal conditions. Fuel cells also have low to zero emissions, more efficiency theoretically than combustion systems due to their non-combustion electrical source of energy, and longer life span than batteries because of its higher energy density (1).

There are five main types of fuel cells: Alkaline, Phosphoric Acid, Molten Carbonate, Solid Oxide, and Proton Exchange Membrane. The main differences among them are the electrolyte mediums and operating temperature for each fuel cell, and each has its own advantages and disadvantages. For example, Alkaline Fuel Cell (AFC) has aqueous potassium hydroxide, an alkaline medium, as its electrolyte whereas Proton Exchange Membrane (PEM) has an acidic medium of usually polyperflouro-sulfonic acid. Because of the alkaline electrolyte, AFC has high performance due to the fast cathode kinetics but has expensive removal of CO_2 from fuel and air streams (1,4). As for PEM, its advantages include low operating temperature of

80°C, quick start up, light weight, compactness, comparatively high efficiency at 40-60%, and reduction of corrosion and management problems (1,4,5). Consequently, PEM is considered to be the best type of fuel cell as the vehicular power source. It is also the fuel cell system our research group is working on.

PEM functions like an electrochemical battery, generating electricity from an oxidation reduction reaction with oxygen and hydrogen as reactants. The oxidation takes place at the anode, and reduction takes place at the cathode, with both anode and cathode separated by Proton Exchange Membrane, hence the name of the type. Oxygen would flow into the fuel cell in one end, and hydrogen would flow into the other end. Hydrogen would then participate in the anode reaction at the anode and split into protons and electrons. The electrons would flow into a load and produce a current from the anode to the cathode, and the protons would pass through the selective membrane to the cathode to participate in the cathode reaction with Oxygen to form the products. The reactions are shown below, with cathode reaction being the limiting half-cell reaction from kinetics (6). The voltage values are referenced to a hydrogen electrode of 0V.

Anode Reaction: $2H_2 \rightarrow 4H^+ + 4e^-$ $E° = 0V$
Cathode Reaction: $O_2 + 4H^+ + 4e^- \rightarrow 2H_2O$ $E° = 1.229V$
Side (unwanted) Cathode Reaction: $O_2 + 2H^+ + 4e^- \rightarrow 2H_2O_2$
Overall Cell Reaction: $2H_2 + O_2 + 2\ H_2O$ $E° = 1.229V$

However, not all of the energy from the reaction is achieved. One of the main loss of efficiency of PEM is activation loss partly because of the low operating temperature. To reduce activation loss, catalysts are being used and researched. Platinum catalyst is currently the most efficient and prevalently used catalyst for PEM oxygen reduction reaction (ORR). However, the scarcity, high cost, CO poisoning, and poor long-term stability of platinum catalysts make it non-feasible for large scale commercialization (7,8). Since Platinum is a rare earth metal with limited

reserves, high demand of it increases its cost. Platinum catalysts are also poisoned by carbon monoxide that constitutes 1-3% in mixture of H_2 gas produced commercially through the steam reforming light hydrocarbon process. Lastly, platinum catalysts have low durability or low activity after a certain period of use (9,10).

Our research is to find a replacement catalyst for platinum that can be commercialized in the future. We are looking for a non-platinum catalyst that not only has as high an activity as Pt catalyst, but also low cost of synthesis, high immunity to poisoning agents, and high durability. The two types of catalysts we are researching on are CNx and FeNC. CNx is a carbon based catalyst with varying amount of nitrogen content, and FeNC is also a carbon based catalyst with varying amount of nitrogen content but with an iron center (11-14).

2. Literature Review

2.1 Carbon Catalysts

Of the non-platinum efficient, low cost catalysts, carbon based catalysts such as carbon nanotubes, carbon nanofibers, graphene, and mesoporous carbon exhibit excellent electrochemical performance during ORR in terms of catalytic activity and practical durability. (5,15-18). Many of these carbon catalysts are also immune to CO and most other chemical poisonings (15-16). However, the activities of these catalysts are high usually in alkaline mediums and much lower in acidic mediums. Since PEM fuel cells operate under acidic mediums, it is imperative to find catalysts that hold higher activity in acidic mediums (17). Of the carbon based catalysts, one type of carbon catalyst that yielded significantly higher catalytic activity than others in acidic medium was the N-doped carbon catalyst (5,17-18).

2.2 N-doping

Many research groups have shown that N-doped carbon catalysts resulted in higher activities. Their carbon materials and nitrogen dopants varied. One doping method involved sulfuric acid, nitric acid, and ammonia heat treatment, a method that has a simple production and low cost (17). Few other nitrogen dopants used are pyrazine and benzylamine, with pyrazine researched to be more efficient in doping nitrogen elements into carbon catalysts (19). It shows that N dopant matters when doping into certain carbon material structure (19).

The reasons for higher activity in N-doped carbons than non-doped carbons were explored. Some reasoned that N-doping leads to increased surface wettability, catalyst diameter reduction, porosity in catalyst structure, more exposed edge planes, and higher proportion of Pyridinic Nitrogen (17). Higher wettability, or the ability for fluids to maintain contact with solid

catalyst particles, can lead to higher oxygen adsorption and possibly higher electron flow. Diameter reduction, increased porosity and exposed edge planes can also increase the adsorption of oxygen to the catalyst, leading to increased cathodic catalytic activity. As for Pyridinic Nitrogen, it is one of the three possible forms (Pyridinic, Pyrrolic, Graphitic) of nitrogen-carbon structures shown in Figure 1 (17).

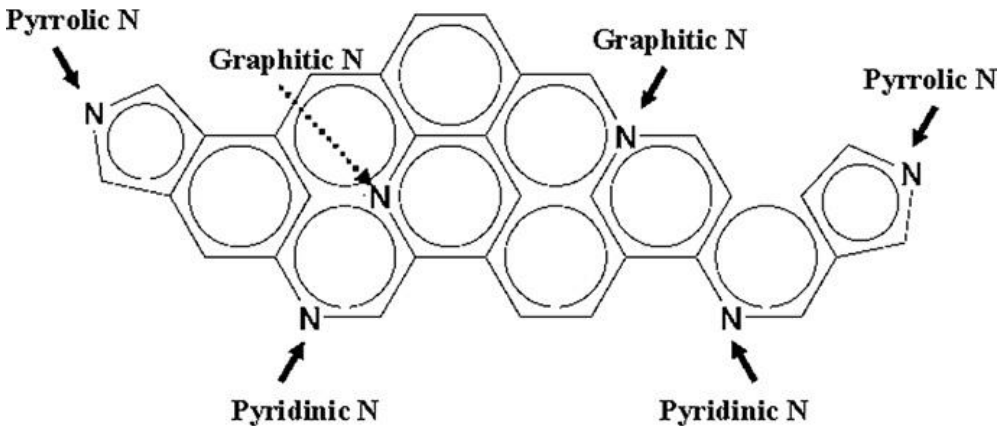

Figure 1: Bonding configurations for nitrogen atoms in N-doped carbon materials (17)

The Pyridinic N, which bonds to 2 carbon and one P-electron to π system, is located near the edge along with Pyrrolic N. The Graphitic N or Quaternary N is located more inside the carbon chain and has 3 carbon bonds. It is also the most desired form because it has higher activity with larger limiting current density than Pyrrolic or Pyridinic N (20). Although higher Graphitic N is desired more than Pyridinic N, Pyridinic N nevertheless is still desired as it also positively affect activity (20). Some reports found higher pyrrolic N as the catalyst surface N content increased, which also resulted in better crystallinity and better activity indicated by higher onset potential, peak current, and steady state diffusion current density (17). Some others reported that outer n-doped graphitic N along the edged structure yielded improved ORR activity (18). However, they also reported that graphitic N just beneath the catalyst surface can undergo

change to a more pyridine like structure, complicating the validity of graphitic N being the major active site (17). Overall, it is concluded that Pyridinic-N and Graphitic-N are considered active sites for ORR in metal-free N-doped carbon materials (17).

ORR is an electron transfer process that is strongly dependent on the electronic structure of catalysts (17). The structural changes caused by N-doping both inside and on the surface of the carbon chain allows for charge delocalization, resulting in positively charged carbon as part of the active site in acidic mediums (5). It was found that oxygen has more negative charge and carbon has more positive charge from XPS spectra results during ORR (17). The positive charges of carbon attract the negative charges of oxygen, inducing ORR. Also it is proposed that N doping increases n-type conductivity of carbon as nitrogen magnifies the SP2 carbon structures which is a good electron conduction system (20,21).

MnOx-CNT, similar to N-doped catalysts, was researched to explore N-doping phenomenon. The results showed that structural strain caused by larger atomic size than carbon facilitates charge localization and associated chemisorption. Highly positive charge on CNT surface was believed to be the catalytically active, further supporting the charge delocalization theory (20).

Nitrogen-doped catalysts not only have high activities, but also have high stability and selectivity. Reports compared stability of N-doped catalysts to Pt catalysts and reported N-doped catalysts have higher stability of 65% retention of the current density after long time of running experiments compared to only Pt catalysts' 56% (17). For selectivity, N-doped catalysts showed higher selectivity for the reaction in which water is formed as the product instead of the side reaction in which hydrogen peroxide is formed as the product (18,20). The reaction in which water is formed as the product is also denoted as the $4e^-$ reaction pathway and the side reaction is

denoted as the $2e^-$ reaction pathway. One of the reasons for high selectivity is that Pyridinic N along the edges has 4 electron lone pair sites due to π electron delocalization, which leads to preference for the $4e^-$ reaction pathway (18).

Overall, N-doping demonstrated higher catalytic activity, while controlling catalyst structure, surface area, and different dopant processes are also important.

2.3 Other Heteroatom Doping

With N-doping proving to be effective in raising activity, other elemental doping and heteroatom doping have sparked interest. Heteroatom doping is the doping of more than one element into a base carbon. Sulfur, boron, and phosphorus doping have sparked interest because of their similar elemental properties to nitrogen such as electronegativity and electron donating ability.

Heterodoped sulfur and nitrogen carbon catalysts resulted in higher activity that was indicated by higher onset potential (21,22). A strong reason sulfur was used is that it exhibits one of the highest hydrogen uptake densities for amorphous carbons because it induces stronger interaction between carbon and hydrogen, which can lead to further charge delocalization (22). Sulfur doping on carbon through dopants such as cysteine which has both nitrogen and sulfur elements can result in sulfonate or sulfate forms in the carbon matrix. The nitrogen in heterodoped catalysts caused similar effects to regular monodoping of nitrogen (21). Together, nitrogen and sulfur heterodoping further increased the catalytic activity from mono-nitrogen doped carbon catalysts (10). It was also noted that adding albumin to precursor mixture changed the morphology of S-N-doped Carbon to an aerogel-like monolithic (single layered) structure with high surface area of 321m^2/g, which can increase adsorption and activity (10).

Heterodoped boron and nitrogen carbon catalysts also exhibited high activity indicated by higher onset potential and higher kinetic current density (10,22). One reason is that adjacent N and B atoms could facilitate charge transfer between neighboring carbon atoms, likely increasing the conductivity of the carbon structure (10). Another reason is that boron itself has lower electronegativity (2.04) than carbon (2.55), leading to a negatively polarized carbon with a positively polarized boron, which attracts negatively polarized oxygen atoms during ORR chemisorption (22). Higher ORR chemisorption would increase the activity of ORR. One other reason is that structurally boron treated carbon catalysts shows an increase in the portion of pyridinic N sites, which help increase activity as they are likely the active sites (20).

Not only do carbon catalysts heterodoped with nitrogen and either sulfur or boron show higher activity than monodoped nitrogen catalysts, they also generally have high selectivity and high tolerance to impurities. It was reported that sulfur nitrogen doping promotes $4e^-$ pathway because of increased spin density in S doped graphene, thereby increasing selectivity (22). It was also reported that boron nitrogen doping resulted in good tolerance to methanol and carbon monoxide in alkaline medium (10).

Heteroatom doping shows great potential in furthering the increase in catalytic activity of carbon catalysts while maintaining high selectivity and immunity. However, the amount of dopants used in heterodoping matters, because too much heterodoping would result in high non-catalytically active defects, increasing the resistance to conductivity or lowering the generated current, indicating lower activity (21). Therefore, finding the optimal amount of doping is essential. One heteroatom doping that interests our group is phosphorus with nitrogen heterodoping that we will address in our experiment on our carbon catalysts.

2.4 FeNC:

Our Catalysts are of two types, FeNC and CNx. FeNC is a nitrogen doped carbon based catalyst that has iron as its metal center, and CNx is another nitrogen doped carbon based catalyst of different structure than that of FeNC.

From previous reports, among non-precious metal catalysts, N, Fe-codoped carbon-based (Fe/N/C) catalysts are some of the most promising candidates because they exhibited high ORR activity in both acidic and alkaline medium (23-25). Other transition metals were explored, but among them (Mn, Fe, Co, Ni, and Cu), Fe, N-heterodoped catalysts exhibited the highest ORR catalyst activity, which fully displayed the importance of Fe-based catalysts in ORR (26). Just like nitrogen heterodoping, there is an optimal amount of iron to be added. Electrochemical measurements revealed that Fe/N/C with an iron content of 0.24 % prepared at 800 °C resulted in catalyst with the optimal activity indicated by high positive onset potential (0.98 V vs. RHE), higher diffusion-limited current, higher selectivity, and higher stability in 0.1 M KOH (6).

Structurally, iron doping resulted in Fe_3C center on carbon, which has high ORR activity due to activation of surrounding graphitic layers that makes outer surface layer active towards the ORR (27). Iron combined with nitrogen doping structurally leads to different iron nitrogen sites that are even better than Fe_3C sites, with FeN_4-like and N–FeN_{2+2} sites being found catalytically ORR active (27). FeN_4 is shown in Figure 2 , while N–FeN_{2+2} is shown in Figure 3, both of which are found in 1, 10-phenanthroline like structures (27). Phenanthroline like structure also helps in adsorbing iron ions because iron is stabilized by at least two pyridinic nitrogens (27). Hence 1, 10-phenanthroline is a precursor we use to synthesize our FeNC catalyst.

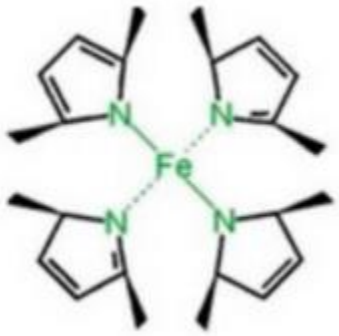

Figure 2: FeN_4 Structure (27)

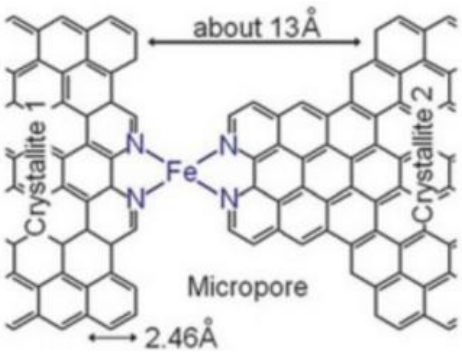

Figure 3: FeN_{2+2} Structure (27)

The active site of FeNC is favored to be an N-stabilized metal center that could be either Fe-N_{2+2} or Fe-N_4 or a mix of both, although some others believe iron is only used as a growth support during FeNC synthesis (14). To test such notion, if iron centers were indeed the active site, the use of known poisons for iron catalysts should lead to significant activity loss in ORR. Sulfur, a known iron poison that readily binds to heme group, decreases activity of FeNC catalysts, so sulfur poisoning of FeNC indicates that the active site contains iron (12). However, FeNC with sulfur has lower pyridinic N which also indicates lowered activity. Therefore, activity loss may be due to both lower pyridinic N and disruption of iron center active site, but there is no conclusive knowledge of the major cause of loss of activity (12). One other support for Fe centered active site is that the activity of FeNC is lowered by acid washing because it washes away Fe which is a vital part of the active site (13).

FeNC is researched right now not only because of its high activity in acidic medium, but also because of its resistance to poisoning, and selectivity. FeNC is slightly poisoned by CO, a poison of Pt catalyst, and its Fe-N_4 clusters could promote $4e^-$ pathway in ORR, increasing selectivity (27,28). However, it does have one drawback, and that is its mediocre durability. It was reasoned that iron was lost from the Fe-based catalyst into the electrochemical environment during the ORR, which can lead to disruption of Fe-N_{2+2} and Fe-N_4 coordination active sites that readily absorbs oxygen, ultimately leading to a reduced activity after a duration of use (28). Further research is needed to improve FeNC stability.

2.5 CNx

CNx, a carbon base with x amount of nitrogen, was inspired by nitrogen doping of carbon catalysts, which reached high catalytic activity. Metal supports involving Fe or Co showed high ORR activity (14,29). The Fe metal particles was reasoned to serve as a catalyst for the formation of the edged carbon nanostructure of the CNx, and as part of the active site (30,31). It was suggested that Fe or Co can stimulate growth of more edged structured CNx, which could result in more pyridinic nitrogen content (14,29). CNx with a higher pyridinic-N content and usually more exposed edge planes is more active. On the contrary, edge planes with no nitrogen content had no ORR activity (14). Consequently, we used Iron(II) Acetate as metal support for a more active CNx. Another support, MgO, can also help yield high nitrogen content and more structured carbon catalyst (29,31). It also is good for leaching out metals such as iron during acid washing (14). Consequently, we use Magnesium Oxide with Iron Acetate as support for CNx catalyst to grow on.

However, there was also significant activity increase for CNx catalysts grown over alumina support with no metal doping. This result was significant in showing that ORR activity can be achieved without a metal as a support (14).

For the active sites of CNx, they are inferred to be much like the N-doped carbon active sites. Cyanide, a known iron poison, was introduced to CNx and resulted in no change in activity (11). Therefore, CNx does not have metal center active sites (11). H_2S was also introduced to CNx and resulted in higher pyridinic N that led to higher activity (12). It was proposed that H_2S increased the pyridinic N sites, which are active sites. Acid washing was done on CNx and resulted in higher activity (13). Results from acid washing showed that nitrogen content were closer to graphitic N than pyridinic N type, which makes sense in that graphitic N is more active than pyridinic for ORR (13).

CNx is also researched right now because of its resistance against impurities such methanol and its high durability (32). The downside is that it has slightly lower activity than FeNC. Nevertheless, both FeNC and CNx have strong potential for future research although they have different active sites and are made of different materials.

2.6 P-doping

Heteroatom doping involving phosphorus holds promising potential in increasing catalytic activity. Studies have shown that N, P doping, B, P doping, and S, P doping on carbon catalysts resulted in more selectivity and higher activity (5,9,19,33,34).

For B, P heterodoping on graphene, a carbon material that has 2d-sp2 structure and high surface area, the dopants used were boric acid for boron and phosphoric acid for phosphorus. Additionally, B-N-P doped graphene exhibited slightly higher activity than B-N doped graphene with an onset potential of 0.9 V in acidic environment (33).

Additional P-S doping to N-doping also yielded higher activity than regular N doping for ORR in acidic mediums. The dopants used were phosphoric acid for phosphorus and cysteine for sulfur. Synthesis involved growing of nitrogen-carbon substrate through pyrolysis on a support, then doping, and then acid washing that is for the purpose of removing metallic compounds on the surface. The results showed an increase of pyridinic N through XPS surface analysis, and increase in catalyst surface area (9). The results also showed that structurally most phosphorus content were on the surface and not in the carbon lattice. As for sulfur, it was present more in the carbon lattice indicated by many C-S-C type bonds through XPS (9).

Heterodoping of N, P led to high activity as well (5,34,35). However, just like most other doping, too high amount of phosphorus doping would lead to lower activity because of destruction of carbon network that provides effective path of electron movement (5). One study of N,P heterodoping on carbon multiwalled nanotubes by using toluene and triphenylphosphine (TPP) as dopants for nitrogen and phosphorus respectively resulted in higher activity than N-doping (34). The varying percent weight of TPP was done to find the optimal phosphorus doping amount. Another parameter, temperature, was assessed and the optimal temperature was found as too high of a temperature would cause larger diameter and reduction of the contacting surface area during ORR, thus reducing activity (34). The XPS results showed phosphorus was strongly incorporated into the carbon matrix shown by XPS data of different P-C bonds (34). Lastly, the catalyst also showed high durability, as the measured current and onset potential maintained much of the original's after 10000 cycles of experimental use (34).

The amount of phosphorus doping is a key factor. One study reported an optimal phosphorus doping of 1.64% by weight in a doping of carbon xerogel using phosphoric acid (35). Another reported optimal phosphorus doping using very low concentration of TPP as

dopant (19). Lastly, phosphorus doping done on nitrogen doped carbon showed that significant differences were observed in activity when Fe/P ratios were changed (14).

Generally, individual separate doping activity strength on carbon catalysts would be in the following order from least to greatest: N-doping < B-N doping < P-N doping (33). We believe N-P doping on either our CNx or FeNC at a small optimal doping amount would yield higher activity.

3. Experimental Methods

3.1 FeNC Synthesis

For our synthesis of FeNC, we have four steps: Wet Impregnation (WI), Ballmilling, Argon heat treatment, and Ammonia heat treatment. WI is the synthesis of carbon-nitrogen-iron catalyst precursor. Ballmilling is the grinding of the precursor to more fine particles yield higher surface area (15). Argon heat treatment is the heating of the sample at a high temperature using an inert gas as high heat is believed to cause micropores in carbon which increases activity (15). Ammonia heat treatment is to additionally dope nitrogen under high temperature.

During WI, used a solvent ratio of 2:1 distilled water to ethanol with a total volume of 150ml. We first added to the solvent 500mg of 1,10 phenanthroline, which is a carbon nitrogen precursor that would fill the pores of black pearls discussed in the theory section. Then we added 31.145mg of iron acetate that gives 1% of iron in solution by weight. Lastly, we added 500mg, the same as phelanthroline, of Black Pearls 2000, which carbon with very fine particle size, and super high surface area. The solution was then heated and stirred in a water bath at 70° C to induce mixing of the materials. Once all of the ethanol and some water are evaporated, leaving with around a third of the original volume, we dry the solution in an oven overnight at 90°C.

During Ballmilling, we used 20 steel balls per 1 gram precursor, and poured both the steel balls and precursor in a ballmilling jar. Before we spin the jar in a ballmilling machine, we flowed nitrogen, an inert gas, into the jar for 15 minutes to displace the oxygen present in the jar. Leaving oxygen in the jar can potentially cause unwanted oxidation reaction to our catalysts at high spin frequency. Then, the jar was rotated for 3 hours at 200rpm. Lastly, we took out the fine powdered precursor out of the jar.

During argon heat treatment, we evenly spread out the precursor from ballmilling onto a quartz boat and placed the quartz boat in a glass tube with the center inside the furnace shown in Figure 5. However, the quartz boat was only set at the edge of the tube and not in the furnace. We follow the steps in Figure 4.

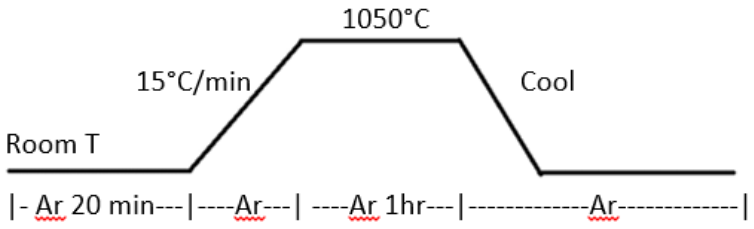

Figure 4: FeNC synthesis: argon heat treatment steps

Argon was initially flown into the glass tube for about 20 minutes from one side to the exit side to displace all of the air in the tube. After, the furnace was ramped up to 1050°C at a pace of 15°C/min while the flow was still in argon. Then the catalyst in the quartz boat was pushed into the center of the furnace using magnets both outside and inside of the tube, and heated for 1 hour exactly. The furnace was cooled after.

Figure 5: Heat Treatment Setup

During ammonia treatment, argon was initially flown into the glass tube to purge out the oxygen originally tube. Then, the furnace was ramped to 950°C at a pace of 15°C/min under argon. After reaching stabilizing 950°C, we switched flow from argon to ammonia and let flow for about 30 minutes to displace the argon in the tube. Then, in a saturated ammonia environment, we pushed the catalyst into the center of furnace and let heat treatment take place for 20 minutes exactly. After, we let the furnace cool and took out the finished product catalyst FeNC.

We tried different ways to successfully dope phosphorus into FeNC. In one way, we incorporated the doping in the ballmilling step of FeNC. All the steps of the ballmilling were the same, but varying amounts of TPP was added to the jar along with the precursor and balls before spinning of the ballmilling jar in the ballmilling machine. In another way, we changed the WI step by adding varying amounts of phosphoric acid to the 2:1 dilute water to ethanol solution.

The phosphoric acid can increase pore size and surface area because it can induce carbon activation (35).

3.2 CNx Synthesis

For our synthesis of CNx, we divided it into 4 steps in consecutive order: incipient wet impregnation (IWI), ballmilling, chemical vapor deposition, and acid washing. IWI is used to make an iron doped metal oxide support for the catalyst to grow on. Ballmilling is used to increase the surface area of the catalyst. Chemical vapor deposition is the growing of the CNx catalyst on the support. Acid washing is the final step to remove metal oxide support from the catalyst, leaving only inactive iron that is encased in carbon support.

During IWI, we used 2g of MgO as support. We also used 124.6mg of iron(II) acetate for 2% of iron by weight, and mixed that with 130ul of water to dissolve the iron(II) acetate. The specific volume of water was determined by the pore volume of the MgO which is 65ul/g. The iron(II) acetate water solution is then impregnated on MgO in small portions at a time, yielding Fe/MgO.

During ballmilling, we used 20 steel balls per gram precursor, and poured both the steel balls and precursor in a ballmilling jar. Before we spin the jar in a ballmilling machine, we flowed nitrogen, an inert gas, into the jar for 15 minutes to displace the oxygen in jar. Leaving oxygen in the jar can potentially cause unwanted oxidation reaction to our catalysts at high spin frequency. Then, the jar was spun for 3 hours at 200rpm. Lastly, we took out the fine powdered precursor out of the jar.

During chemical deposition, we placed FeMgO in the furnace. We first flushed out the oxygen in the quartz tube with nitrogen. After we ramped the system to 900°C in nitrogen

atmosphere at 10°C per minute. Then we flushed CH_3CN (methyl cyanide) onto the FeMgO support at 900°C for 2 hours.

During acid washing, we mixed HCl (1M) with catalyst from the chemical deposition in a heated water bath of 60°C for 1 hour. The liquid part of the solution was filtrated using filtration paper and filtration funnel. Excess water is added to wash off the acid that may stick on the catalyst. The catalyst on the filtration paper is then put in beakers, left to dry in the oven over at night at 70°C.

For phosphorus doping, we added varying amounts of TPP depending on the P/Fe ration to the IWI precursor in the ballmilling stage. The result would give us a FeMgO-P support that would incorporate P onto the CNx catalyst grown on the support.

3.3. Activity Testing

For either testing of CNx or FeNC with P-doping, we first turned the fine solid catalyst particles to liquid ink that can be applied to the RDE/RRDE testing apparatus that is suspended on top of the solution container shown in Figure 6. We added 5mg of catalyst and 48ul of Nafion and 175ul of ethanol that would optimally disperse the catalyst. Nafion is used as a proton-transfer electrolyte in acidic environment and can enhance adhesion to disk surface (glassy carbon) of the testing apparatus (5,17). The dissolving is enhanced by long period of sonication, during which the catalyst solution in a vial is motioned by the currents from the sonication machine hitting the vial.

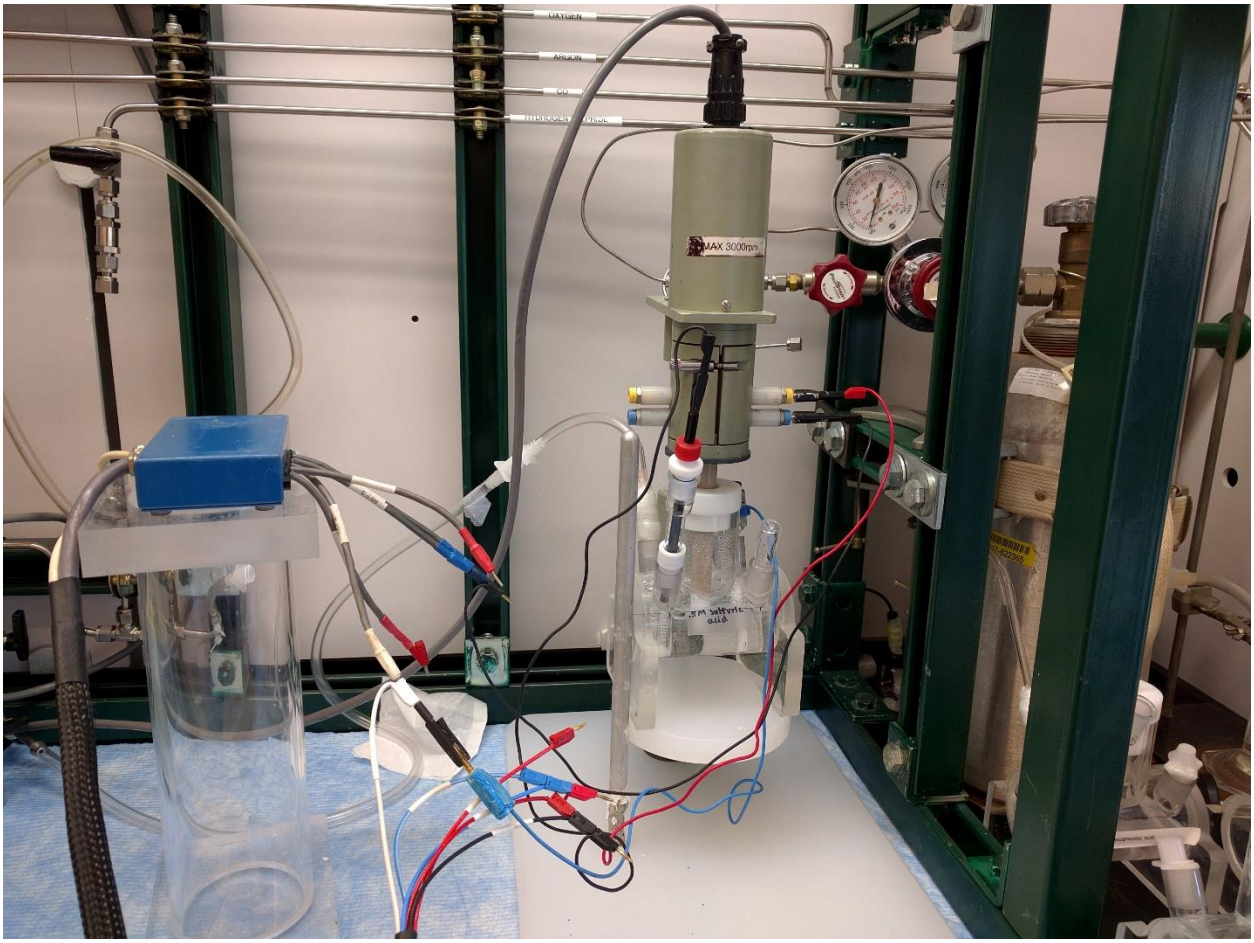

Figure 6: Half Cell Testing Apparatus set up

After the catalyst ink was prepared, optimal amount of 9ul of ink was loaded to the GC disk of the apparatus using the pipette and left to dry. The half-cell, specifically at the cathode side of the fuel cell reaction, was set up by having 0.5M sulfuric acid in a container, apparatus on top of the container with the disk insert into the solution, wires of different electrodes connected from the potentiostat (applies voltage), and flow tube inserted into the solution, all shown in Figure 6.

The different electrodes connected are counter, working (includes ring), and reference electrode. Counter electrode is used to close the current circuit in our half-cell. The reference

electrode (hydrogen electrode) is used for a point of reference for potential measurement and has a stable electrode potential. The working electrode is the electrode on which the reaction is occurring. In potentiostatic mode, our RDE apparatus will accurately control the potential of the Counter Electrode (Pt coil) against the Working Electrode (GC) so that the potential difference between the working electrode and the Reference Electrode (Hydrogen) is well defined (34,36).

Oxygen was flown into the solution to saturate it with oxygen. Then, activity tests, specifically RDE were run to generate CV curves at a specified rpm through rotating the disk. The first 2-3 scans are fast CV scans to reach electrical stability in the solution, given that the first few CV curves matches. After electrical stability was reached, slow CV scans were done at different rpms. The high voltage potential region of the CV curves of slow CV scans at different rpm should match, although the lower potential region would be different because of different limiting current from different rpms causing different oxygen diffusion rate. After flow is switched to argon from oxygen and let argon to saturate the solution for 15 minutes. The fast CVs were run to electrically stabilize the system and a slow CVs was run at any rpm (would be same at any rpm) to serve as the background CV. The actual CV data would be oxygen CV data minus the Argon background CV.

Overall, the RDE activity testing can be summarized in the follow order: Catalyst to Ink → Ink on GC disk of the apparatus → Apparatus with dried ink suspended on top → the GC disk inside the acidic solution → Counter and reference electrodes inside solution → Flow tube (oxygen/argon) inside solution → Rpm machine connected to apparatus → electrodes connected to apparatus → oxygen flow to saturation → Fast oxygen CV scans → slow oxygen CV scans → Argon flow to saturation → fast and slow argon CV scans

Other pertinent experiments that were not my focus but would help for the analysis are X-ray diffraction, Brunauer-Emmett-Teller (BET) analysis, Raman spectroscopy, X-ray photoelectron spectroscopy (XPS) and scanning electron microscopy (SEM), RRDE. X-ray diffraction shows crystal structure for analysis. Surface area and pore size distribution can be calculated through BET analysis. Morphology and composition of catalyst can be determined by SEM and Raman spectroscopy, with SEM more focused on surface and Raman more focused on the interior structure (19,34). XPS, can show types of bonding at the surface or the successfulness of the doping. Lastly, RRDE can find the selectivity of the catalyst by finding the number of electrons for either 2 e^- or 4 e^- pathway. The number of electrons can be found using Levich slop from Levich plots from different rpm (34,35).

For measures of activity using CV from RDE, we can use onset potential, half-wave potential, or limiting current for a constant rpm. Also the area under is the CV curve is correlated with capacitance which can be a consideration for activity. Onset potential and limiting current can be found by looking at the CV curve, with onset potential being the potential at which current sees huge drop (I/A = -.1) and halfway potential being the potential at the current between the starting current and limiting current, and limiting current being the largest unchanging current possible on the CV curve. We will be using primarily onset potential for comparing activity of different catalysts.

4. Results and Discussion

4.1 FeNC P-doping

We tried two ways to dope phosphorus into FeNC catalysts. The first way involved mixing phosphoric acid in the WI step and the results are shown in Figure 7.

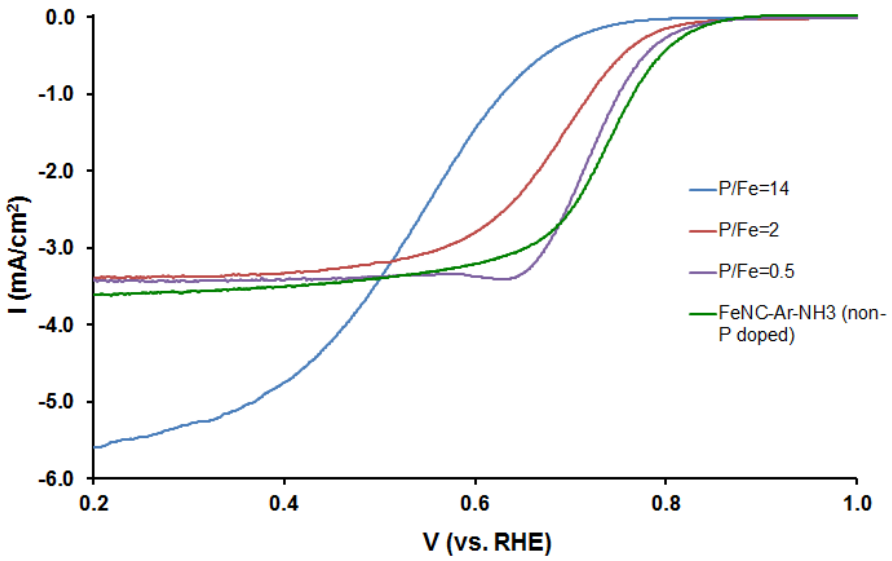

Figure 7: P/Fe ratio P-Doping through phosphoric acid on FeNC polarization graph

The CV scans were ran from 1.2 V to 0 V. The 1.2 V is the initial and also the theoretical voltage of the ORR. As the voltages lower than theoretical voltage were applied to the reaction, cathodic current (negative) is generated from cathode reaction at the working electrode to the solution to induce reduction (37). The voltage at which the current is initially generated is known as onset potential, and the higher the onset potential, the higher the activity as the voltage is closer to the theoretical voltage (37). Since the voltage initially generated is very small, we use -0.1mA/cm^2 as the approximate initial current density. From Figure 7, the non-doped FeNC has

the highest onset potential, whereas the P/Fe = 14 FeNC has the lowest onset potential. P/Fe = 0.5 FeNC has the highest onset potential out of the all of the P/Fe dopings. The limiting current is highest current, and can will change with different rotation speed as the limiting current is also a function of the rate of mass transport. P/Fe =14 FeNC has the highest limiting current and the others have lower limiting current. The half-wave potential is potential at a current halfway between initial current and the limiting current, and higher half-wave potential corresponds to better activity. P/Fe = 14 FeNC has the lowest half-wave potential. We compared the onset potentials of P-doping on FeNC to find the activities shown in Figure 8 as onset potentials are accurate indicators of activity.

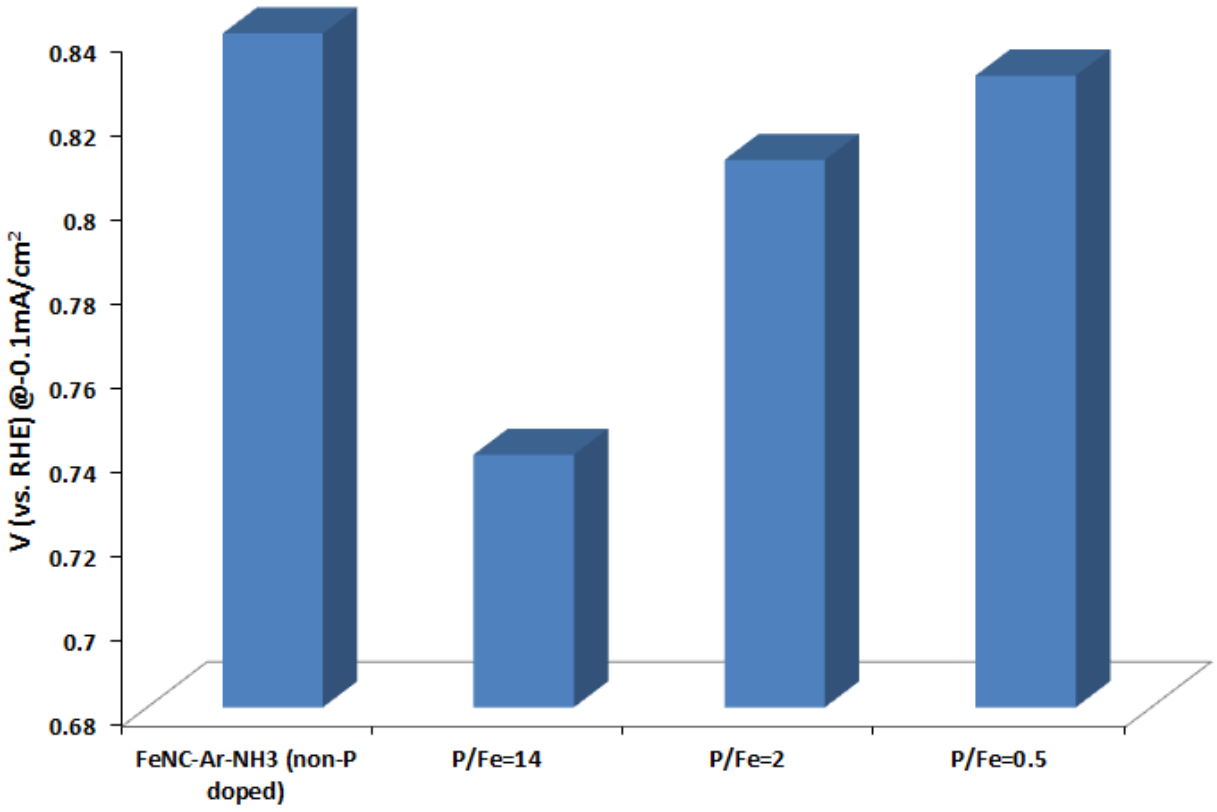

Figure 8: Onset potentials of FeNC P-doping

However, we cannot conclude that phosphorus doping has no increasing effect on activity of FeNC catalysts because phosphorus may not have been incorporated successfully into the FeNC both on the inside and surface of the iron centered carbon matrix. Therefore, we tried another way of incorporating phosphorus into FeNC using TPP in the ballmilling step. The results of using TPP showed similar results to that of using phosphoric acid. Since another way of incorporating phosphorus through using TPP also didn't show higher activity, it can be concluded that phosphorus doping on FeNC does not increase activity.

4.2 CNx P-doping

CNx and FeNC are different catalysts, and P-doping on CNx showed promising results. Different ratios of P/Fe P-doping were done on CNx through TPP, and results in the form of RDE CV graphs were shown in Figure 9. The onset potential and half-wave potential from CV graph of the P/Fe = 2 CNx were higher than those of the non-doped CNx, indicating higher activity. The onset potential was higher by approximately 50 mV and the half-wave potential was higher by approximately 130 mV.

However, the onset and halfway potentials of P/Fe = 1 CNx were similar to those of the non-doped CNx. It showed that there is an optimal amount of P-doping to achieve to higher activity, and that optimal amount is around P/Fe of 2. It is noted that higher P/Fe ratios have not been tested.

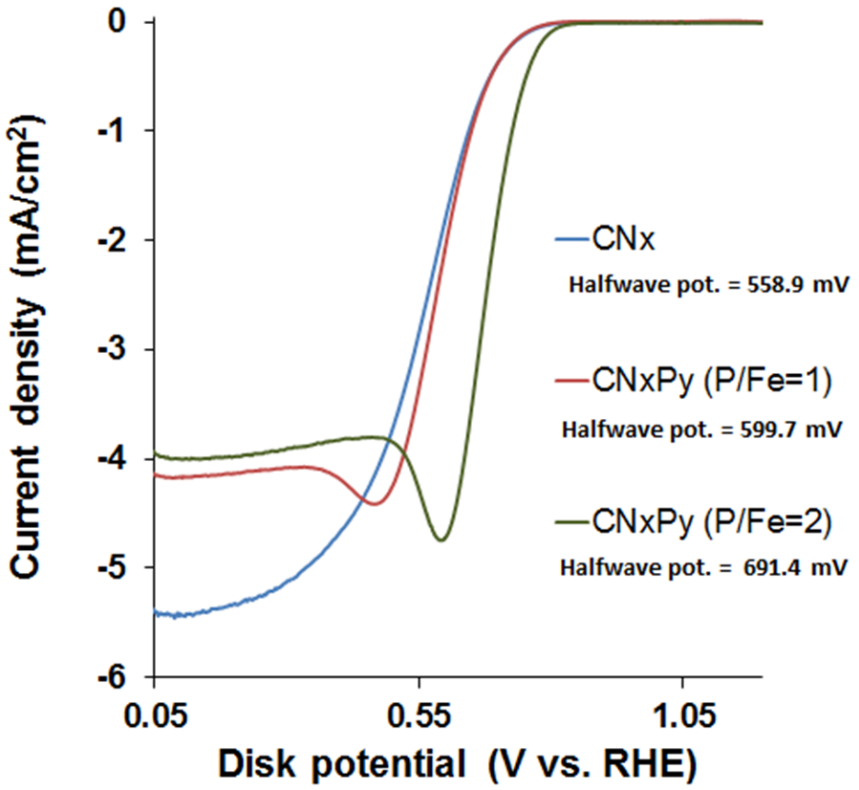

Figure 9: CNx P/Fe ratio P-doping polarization graph, data obtained by Kuldeep Mamtani

The increased activity for phosphorus doping on CNx can be explained by some of the following causes. Research found that P-doping modifies the morphology of catalysts to uneven surfaces with more open edge sites, increasing catalysts surface area and pyridinic nitrogen content (5). Just like N-doping, P-doping can also enhance charge delocalization and asymmetric spin and charge density, increasing the active sites for oxygen adsorption and the overall ORR activity (5,9,20,22,33). Although phosphorus (2.19) is less electronegative than carbon (2.55), the enhanced asymmetric spin and charge density on the carbon by phosphorus weaken the O_2 bond and strengthen adsorption of oxygen molecule on carbon atoms during catalytic activity (9). P-doping on CNx could further enhance charge delocalization, spin density and oxygen adsorption. P-doping on FeNC may not enhance such because of the phosphorus interaction with

iron and the possibility of reducing the charge delocalization and spin density that iron and nitrogen causes on carbon.

Research shown that phosphorus doping on graphene have increased activity because of possible increased electric conductivity of graphene, modification of graphitic π electron system, and improved donor properties of carbon (20,22,33). XPS and Raman Spectroscopy could be done on the P-doped CNx to see P-C and P-O bonding to support the phosphorus incorporation into carbon matrix and surface. The incorporation of phosphorus in the matrix in CNx could cause change in its π system and graphitic structure, resulting in higher electron conductive carbon structure and higher generated current (35). Since FeNC active sites are more iron-nitrogen involved and less of carbon-nitrogen character, P-doping on FeNC's carbon conductivity may not have much effect on increasing the activity.

5. Conclusions

With an increasing demand for alternative energy, fuel cell catalysts are being researched to achieve higher activity and lower costs. Iron nitrogen carbon (FeNC) and nitrogen carbon (CNx) catalysts hold promising potential for being catalytically active at low costs. Phosphorus were doped on both FeNC and CNx catalysts to improve activity because of phosphorus' elemental properties. Triphenylphosphine was used as a phosphorus dopant and incorporated in the ballmilling step for both FeNC and CNx synthesis. P-doping on FeNC showed no increase in activity, but P-doping on CNx with a phosphorus to iron ratio of 2 showed a higher activity. This showed that P-doping positively affected a non-metal centered catalyst because of possibly increased adsorption of oxygen and increased electrical conductivity of the graphene carbon like structure and π electron system. This also showed that P-doping may affect metal centered catalyst negatively possibly because of the disruption of the iron carbon structural connections.

6. Future Work

Different tests such as BET analysis, Raman spectroscopy, XPS, and SEM could be done on the P-doped CNx and FeNC to provide structural insight at the atomic level. The structural changes may give clues to the changes in activities. Also other phosphorus dopants can be done on both catalysts to see the effects on the activity and the corresponding structures. The different dopants can lead to a better overall understanding of the catalytic mechanisms and structures of FeNC and CNx in ORR.

Perhaps, structural changes can be achieved through other methods other than doping. One research have shown that more tube like structure can increase surface area and possibly electron flow (22). Another showed that vertical or horizontal alignment in catalyst structure could facilitate diffusion of electrolyte ions and oxygen (10). Similar structural changes can be implemented on FeNC and CNx to improve activity and explore more about the catalysts.

Bibliography

1) Jiangshui Luo; Olaf Conrad; Ivo F. J. Vankelecom. Imidazolium methanesulfonate as a high temperature proton conductor. Journal of Materials Chemistry A1 2013.

2) Steele, B.C.H.; Heinzel, A. Materials for fuel-cell technologies. Nature 2001, 414, 345–352.

3) Higgins, D.; Chen, Z. Recent Development of Non-precious Metal Catalysts. In Lecture Notes in Energy—Electrocatalysis in Fuel Cells; Shao, M., Ed.; Springer: New York, NY, USA, 2013; Volume 9, pp. 247–270.

4) Laraminie, J. and A. Dicks, Fuel Cells Systems Explained, John Wiley & Sons: New York, NY 2000.

5) Chang Hyuck Choi; Sung Hyeon Park; Seong Ihl Woo. Phosphorus–nitrogen dual doped carbon as an effective catalyst for oxygen reduction reaction in acidic media: effects of the amount of P-doping on the physical and electrochemical properties of carbon. J. Mater. Chem., 2012, 22, 12107

6) Jiang, Y.; Lu, Y.; Lv, X.; Han, D.; Zhang, Q.; Niu, L.; Chen, W. Enhanced Catalytic Performance of Pt-Free Iron Phthalocyanine by Graphene Support for Efficient Oxygen Reduction Reaction. ACS Catal. 2013, 3, 1263–1271.

7) Gasteiger, H.A.; Kocha, S.S.; Sompalli, B.; Wagner, F.T. Activity benchmarks and requirements for Pt, Pt-alloy, and non-Pt oxygen reduction catalysts for PEMFCs. Appl. Catal. B 2005, 56, 9–35.

8) Borup, R.; Meyers, J.; Pivovar, B.; Kim, Y.S.; Mukundan, R.; Garland, N.; Myers, D.; Wilson, M.; Garzon, F.; Wood, D.; et al. Scientific Aspects of Polymer Electrolyte Fuel Cell Durability and Degradation. Chem. Rev.2007, 107, 3904–3951.

9) Chang Hyuck Choi; Min Wook Chung; Sung Hyeon Parka; Seong Ihl Woo. Additional doping of phosphorus and/or sulfur into nitrogen-doped carbon for efficient oxygen reduction reaction in acidic media. Phys.Chem. Chem. Phys., 2013, 15, 1802

10) Shuangyin Wang; Eswaramoorthi Iyyamperumal; Ajit Roy; Yuhua Xue; Dingshan Yu; Liming Dai. Vertically Aligned BCN Nanotubes as Efficient Metal-Free Electrocatalysts for the Oxygen Reduction Reaction: A Synergetic Effect by Co-Doping with Boron and Nitrogen. Angew. Chem. Int. Ed. 2011, 50, 11756 –11760

11) D. von Deak, D. Singh, J.C. King, U.S. Ozkan, Use of carbon monoxide and cyanide to probe the active sites on nitrogen-doped carbon catalysts for oxygen reduction, Appl. Catal. B-Environ., 113-114 (2012) 126-133

12) D. Singh, K. Mamtani, C.R. Bruening, J.T. Miller, U.S. Ozkan, Use of H2S to Probe the Active Sites in FeNC Catalysts for the Oxygen Reduction Reaction (ORR) in Acidic Media, ACS Catalysis, (2014) 3454-3462.

13) D. Singh, J. Tian, K. Mamtani, J. King, J.T. Miller, U.S. Ozkan, A comparison of N-containing carbon nanostructures (CNx) and N-coordinated iron–carbon catalysts (FeNC) for the oxygen reduction reaction in acidic media, J. Catal., 317 (2014) 30-43.

14) Kuldeep Mamtani; Umit S. Ozkan. Heteroatom-Doped Carbon Nanostructures as Oxygen Reduction Reaction Catalysts in Acidic Media: An Overview. Catal Lett (2015) 145:436–450

15) Jaouen Frederic; Proietti Eric; Lefevre Michel; Chenitz Regis; Dodelet Jean-Pol; Wu, Gang; Chung Hoon Taek; Johnston Christina. Recent advances in non-specious metal catalysis for oxygen-reduction reaction in polymer electrolyte fuel cells. Energy Environ. Sci., 2011 4 114

16) Yang Zhi; Nie Huagui; Chen Xian; Huang Shaoming. Recent progress in doped carbon nanomaterials as effective cathode catalysts for fuel cell oxygen reduction reaction. Journal of Power Sources 2013 236 238-249

17) Yin, J.; Qiu, Y.; Yu, J.; Zhou, X.; Wu, W. Enhancement of electrocatalytic activity for oxygen reduction reaction in alkaline and acid media from electrospun nitrogen-doped carbon nanofibers by surface modification. RSC Advances, 2013, 3, 15655

18) Kim, H.; Lee, K.; Woo, S. I.; Jung, Y. On the mechanism of enhanced oxygen reduction reaction in nitrogen-doped graphene nanoribbons. Phys. Chem. Chem. Phys., 2011, 13, 17505–17510

19) Jessica Campos-Delgado; Indhira O. Maciel; David A. Cullen; David J. Smith; Ado Jorio; A. Pimenta; Humberto Terrones; Mauricio Terrones. Chemical Vapor Deposition Synthesis of N-, P-, and Si-Doped Single-Walled Carbon Nanotubes. Acsnano 2010, 4 3 1696-1702.

20) Zhi Yang; Huagui Nie; Xi'an Chen; Xiaohua Chen; Shaoming Huang. Recent progress in doped carbon nanomaterials as effective cathode catalysts for fuel cell oxygen reduction reaction. Journal of Power Sources 236 (2013) 238e249

21) Chang Hyuck Choi; Sung Hyeon Park; Seong Ihl Woo. Heteroatom doped carbons prepared by the pyrolysis of bio-derived amino acids as highly active catalysts for oxygen electro-reduction reactions. Green Chem., 2011, 13, 406

22) Jens Peter Paraknowitsch; Arne Thomas. Doping carbons beyond nitrogen: an overview of advanced heteroatom doped carbons with boron, sulphur and phosphorus for energy applications. Energy Environ. Sci., 2013, 6, 2839

23) Chen, Z.; Higgins, D.; Yu, A.; Zhang, L.; Zhang, J. A review on non-precious metal electrocatalysts for PEM fuel cells. Energy Environ. Sci. 2011, 4, 3167–3192.

24) Jaouen, F.; Proietti, E.; Lefèvre, M.; Chenitz, R.; Dodelet, J.-P.; Wu, G.; Chung, H.T.; Johnston, C.M.; Zelenay, P. Recent advances in non-precious metal catalysis for oxygen-reduction reaction in polymer electrolyte fuel cells. Energy Environ. Sci. 2011, 4, 114–130.

25) Xiang, Z.; Xue, Y.; Cao, D.; Huang, L.; Chen, J.-F.; Dai, L. Highly Efficient Electrocatalysts for Oxygen Reduction Based on 2D Covalent Organic Polymers Complexed with Non-precious Metals. Angew. Chem. Int. Ed. 2014, 53, 2433–2437.

26) Peng, H.; Liu, F.; Liu, X.; Liao, S.; You, C.; Tian, X.; Nan, H.; Luo, F.; Song, H.; Fu, Z.; et al. Effect of Transition Metals on the Structure and Performance of the Doped Carbon Catalysts Derived From Polyaniline and Melamine for ORR Application. ACS Catal. 2014, 4, 3797–3805.

27) Liu, J.; Li, E.; Ruan, M.; Song, P.; Xu, W. Recent Progress on Fe/N/C Electrocatalysts for the Oxygen Reduction Reaction in Fuel Cells. Catalysts 2015, 5, 1167-1192.

28) Ferrandon, M.; Wang, X.; Kropf, A.J.; Myers, D.J.; Wu, G.; Johnston, C.M.; Zelenay, P. Stability of iron species in heat-treated polyaniline-iron-carbon polymer electrolyte fuel cell cathode catalysts. Electrochim. Acta 2013, 110, 282–291.

29) P.H. Matter, E. Wang, M. Arias, E.J. Biddinger, U.S. Ozkan, Oxygen reduction reaction activity and surface properties of nanostructured nitrogen-containing carbon, J. Mol. Catal., 264 (2007) 73-81.

30) P.H. Matter, E. Wang, J.-M.M. Millet, U.S. Ozkan, Characterization of the iron phase in CNx-based oxygen reduction reaction catalysts, J. Phys. Chem. C, 111 (2007) 1444-1450.

31) P.H. Matter, E. Wang, U.S. Ozkan, Preparation of nanostructured nitrogen-containing carbon catalysts for the oxygen reduction reaction from SiO2 and MgO supported metal particles, J. Catal., 243 (2006) 395-403.

32) Von Deak D, Biddinger EJ, Ozkan US (2011) J Appl Electrochem 41:757

33) Chang Hyuck Choi; Min Wook Chung; Han Chang Kwon; Sung Hyeon Parka; Seong Ihl Woo. B, N- and P, N-doped graphene as highly active catalysts for oxygen reduction reactions in acidic media. Mater. Chem. A, 2013, 1, 3694

34) Ziwu Liu; Feng Peng; Hongjuan Wang; Hao Yu; Jun Tan; Lili Zhu. Novel phosphorus-doped multiwalled nanotubes with high electrocatalytic activity for O2 reduction in alkaline medium. Catalysis Communications 16 (2011) 35–38

35) Jiao Wua; Zhenrong Yang; Qijun Sun; Xiaowei Li; Peter Strasser; Ruizhi Yang. Synthesis and electrocatalytic activity of phosphorus-doped carbon xerogel for oxygen reduction. Electrochimica Acta 127 (2014) 53–60

36) Metrohm Autolab. Basic overview of the working principle of a potentiostat/galvanostat (PGSTAT) – Electrochemical cell setup. 20 December 2011.

37) Pine research Instrumentation. Hydrodynamic Voltammetry Theory. 2011.